

## DEVELOPMENT AND ASSESSMENT OF MTOR INHIBITORS FOR CANCER TREATMENT: DESIGN, SYNTHESIS, CHARACTERIZATION, AND PHARMACOLOGICAL EVALUATION

Krishna Halkare\*<sup>1</sup>, Parvathi C. V. and Ramesh Hedgapure

Department of Pharmaceutical Chemistry RRK Samithi's College of Pharmacy, NaubadBidar  
– 585402.

Article Received on  
10 Sept. 2023,

Revised on 01 Oct. 2023,  
Accepted on 22 Oct. 2023

DOI: 10. 20959/wjpr202319-30104

### \*Corresponding Author

**Krishna Halkare**

Department of  
Pharmaceutical Chemistry  
RRK Samithi's College of  
Pharmacy, Naubad Bidar -  
585402.

### ABSTRACT

Navigating the intricate world of protein modeling and drug discovery is a journey rife with complex paths and innovative strategies. Homology modeling emerges as a crucial lifeline, enabling the prediction of protein structures when traditional techniques fall short, especially for large proteins beyond the scope of NMR or X-ray diffraction. This process involves seven systematic steps, culminating in model validation. The drug discovery process is an intricate symphony of synthetic chemistry, molecular modeling, computational biology, structural genomics, and pharmacology. It encompasses candidate molecule identification, synthesis, characterization, efficacy and toxicity screening, and a choice between physiology-based and

target-based discovery paradigms. High-throughput screening plays a pivotal role in identifying potential drug candidates, while computational methods, such as computer-aided drug design and structure-based drug design, enrich the toolkit. In this journey, the power of computational methods shines through, offering cost efficiency, the exploration of uncharted chemical space, and the potential to reshape medicine. Molecular docking, pharmacophore mapping, and lead optimization represent key milestones in the pursuit of tailored therapies and medical wonders. Heterocycles, particularly quinoline, play a significant role in this exploration, with diverse applications and a rich historical legacy. The intricate dance of science advances, offering hope for solutions to complex medical challenges.

**KEYWORDS:** Pharmacophore, Molecular dynamics, Homology modeling, Molecular docking.

## INTRODUCTION

Cancer, an insidious condition characterized by the uncontrolled proliferation of abnormal cells, remains a formidable adversary in the field of human health. Its prevalence is striking, with nearly one in three individuals confronting the looming threat of this relentless disease, where cells defy the normal constraints of growth and division. Within each cell, the occurrence of DNA mutations unfolds at an astonishing rate, approximately one in every 20 million per gene per division. Over a lifetime, the human body replaces around 10 million cells per second, culminating in a staggering total of  $10^{16}$  cells.

The origins of cancer often bear the fingerprints of infectious agents, including notorious culprits such as the Hepatitis B virus (HBV), Human Papillomavirus (HPV), and Human Immunodeficiency Virus (HIV). These agents elevate the risk of specific cancers like Nasopharyngeal, Cervical, and Kaposi's Sarcoma. *Helicobacter pylori*, a bacterial villain, further compounds the list by contributing to stomach cancers.

The journey of cancer begins with exposure to carcinogens and mutagens, which are cancer-causing agents lurking in our daily sustenance, water, air, and the chemicals we encounter. As these agents infiltrate the body, epithelial cells, lining surfaces such as the skin and respiratory tract, engage in a relentless battle against the onslaught. Remarkably, over 90% of cancers originate from these epithelial cells, forming a class known as carcinomas. In a minority of cases, genetics tip the scales toward early cancer development, such as in certain childhood leukemias and retinal cancers.

While cancer can strike at any age, it is most prevalent among the elderly, with a staggering 60% of new cancer cases and two-thirds of cancer-related deaths affecting individuals aged over 65. Common cancers like breast, colorectal, prostate, and lung cancers become more prevalent with advancing age. This increase aligns with an augmented vulnerability to the later stages of carcinogenesis due to environmental factors. Hormonal exposure, such as estrogen and testosterone, can also influence cancer risk. Cellular immunity's decline opens the door to immunogenic cancer types like lymphomas and melanomas. With age comes a longer window of exposure for DNA mutations to accumulate, increasing the risk of cancer.

The core traits of cancer, known as hallmarks, encompass six distinctive features: immortality, growth signals, overriding inhibition, evading death, angiogenesis, and metastasis. These traits weave the fabric of cancer's existence, with their prominence varying

depending on the type of tumor.

The complexity of cancer is further underscored by the challenges in developing effective medications. Existing anti-cancer drugs deploy diverse mechanisms of action, exhibiting varying effects on normal and cancer cells. Finding a universal "cure" remains an elusive goal, as cancer manifests in numerous forms, potentially as many as 100 types. Moreover, the subtle biochemical disparities between cancerous and normal cells often hinder the efficacy of anti-cancer drugs, as they can have toxic effects on rapidly dividing normal cells, particularly in the intestines and bone marrow. The adaptability of cancer is another obstacle, as cancer cells initially suppressed by a specific drug can develop resistance, necessitating multi-drug strategies of varying durations.

Most present-day cancer treatments rely on cytotoxic drugs, which are cell-killing agents that interfere with DNA functions. However, these drugs pose significant risks unless they can specifically target cancer cells, a challenge given that cancer cells are mutated versions of our own cells.

In the quest to confront cancer, humanity faces a complex puzzle, emblematic of the intricacies of our biology and the adaptive mechanisms that enable cancer's persistence. Achieving targeted, effective treatments demands scientific innovation and profound understanding, representing an unwavering battle against this formidable adversary.

The diverse faces of cancer, the intricate pathways it follows, and the myriad targets for intervention remind us of the multifaceted nature of this disease. The collective efforts of science, medicine, and humanity continue to push the boundaries of understanding and strive for breakthroughs in the relentless fight against this enigmatic foe.

## **MATERIALS AND METHODS**

### **Homology Modeling**

To construct the 3D structure of the mTOR kinase domain, we employed Biovia Discovery Studio. The Modeler algorithm was instrumental in generating the model using the crystal structure of PI3K gamma (PDB ID: 3S2A) as a template. This crystal structure boasts a resolution of 2.5 Å and is complexed with a quinoline inhibitor. For the human mTOR protein sequence's C-terminal region, we consulted the UniProt database (P42345). Employing the ClustalW program, we executed sequence alignment between mTOR and PI3K gamma to

identify shared regions. The catalytic domains of mTOR and PI3K gamma exhibited up to 45% similarity.

After pinpointing conserved and variable regions, we extracted restraints, distances, and dihedral angles from the template structure, transferring them to the mTOR model. Our stereochemical restraints were acquired from the CHARMM force field, encompassing bond length and bond angle preferences. Further guidance for docking studies came from transferring the quinoline inhibitor from the crystal structure to the mTOR homology model. For refinement, our mTOR model underwent 600 ps of Molecular Dynamics (MD) simulations within an explicit water environment.

Minimization was executed using the Consistent Valence Force Field (CVFF), featuring a van der Waals cutoff of 9.5 Å and a distance-dependent dielectric constant of  $1/r$ . Steepest descents were applied for a thousand steps, succeeded by a thousand steps of conjugate gradients until the root mean square (RMS) gradient dwindled to below 0.001 kcal/mol/Å. Our homology models were encompassed by a 10 Å water layer and subjected to optimization through 2 ns of MD simulations at 300 K. To assess model quality, PROCHECK was brought into play, and a Ramachandran plot revealed that a whopping 97% of residues nestled within the favorable region.

### Drug Design

In the realm of drug development, a drug serves as a small molecule ligand that binds to a specific protein. This binding can either augment the protein's activity (an agonist) or dampen/block its function (an antagonist). A promising approach to unearth potential drug candidates involves exploring how the target protein interacts with various compounds. The process of drug design predominantly falls into two categories: ligand-based and structure-based approaches.

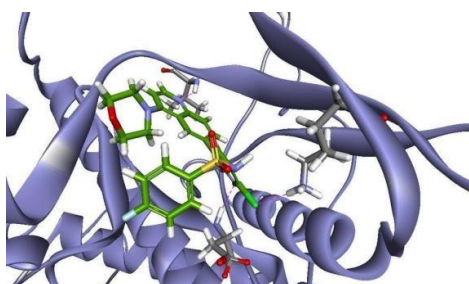


**Fig. 4:** Showcases the Homology Model of Human mTOR intertwined with the ligand gleaned from PI3K gamma. The dotted lines elegantly illustrate interactions with key

**amino acids—Asp 177, Lysine 97, and Valine 60.**

### **Ligand-Based Drug Design**

This approach capitalizes on knowledge about molecules that bind to the target of interest. These existing molecules can help derive a pharmacophore model, outlining the essential structural traits a molecule must possess to engage with the target effectively.

### **Structure-Based Drug Design**

Here, knowledge of the three-dimensional structure of the target protein plays a pivotal role. Techniques like X-ray crystallography or NMR spectroscopy provide insights into the target's structural intricacies. When the experimental structure of the target isn't available, a homology model can be fashioned based on a related protein's structure.

[Include Figure 5 as you mentioned in your original text.]

### **Pharmacophore Studies using Catalyst**

The term "pharmacophore" refers to a molecular framework carrying the crucial features responsible for a drug's biological activity. In the context of drug design, Biovia Catalyst offers a robust toolset for rational design.

### **Chemical Feature-Based Models from Catalyst®**

1. **HipHop:** Generates common feature pharmacophore models from compounds known to be active, even when the exact activity data is absent.
2. **HypoGen:** Constructs SAR hypothesis models using molecules with known activity values on a specific target.
3. **HypoRefine:** Enhances pharmacophore-based 3D QSAR optimization by considering exclusion volumes, leading to more accurate modeling of biological activity influenced by molecular shape.
4. **Exclusion Volume:** This feature adds a layer of specificity by specifying regions in space that must remain devoid of atoms or bonds. It factors in steric hindrance, further refining the design.

With Catalyst®, pharmacophore studies gain a robust toolkit to decipher the intricate dance between molecules and proteins, contributing significantly to the art of drug design.

### **Compare/Fit**

The Compare/Fit feature within Catalyst offers a means to compare and fit compounds and

hypotheses, gauging their degree of similarity in both geometric and functional aspects. In the context of database searches, Compare fits the initial hypothesis onto retrieved hit molecules, scoring them based on their geometrical alignment.

### Cost Parameters

- **Fixed Cost:** Represents the most basic hypothesis that perfectly fits the data.
- **Null Hypothesis:** Implies the cost when each molecule is estimated as having mean activity, essentially suggesting a hypothesis with no features.
- **Error Cost:** Measures the bits required to describe the deviation in the leads. This increases as the root mean square difference between predicted and measured activities for training set molecules rises.
- **Weight Cost:** Reflects the bits needed to depict feature weights.
- **Configuration Cost:** Encompasses the bits necessary to describe feature types and their relative positions in the hypothesis. This fixed cost hinges on the complexity of the hypothesis space being optimized. HypoGen, for instance, assumes that active molecules should map more features than inactive ones, influencing its configuration cost.

### HipHop Model (Qualitative)

- Identifies common three-dimensional arrangements of chemical features shared among molecules in a training set.
- Matches a molecule's chemical features against drug candidates or 3D databases.
- The resultant hypothesis aids iterative searches in chemical databases to unearth new potential lead candidates.

### HypoGen Model (Quantitative)

- Constructs SAR hypothesis models from molecules with known activity values.
- Selects pharmacophores common among active compounds but not inactive ones, refining them through simulated annealing.
- The optimized pharmacophores predict unknown compound activity or search for leads in 3D databases.
- The selection of a training set holds immense importance as hypotheses stem directly from this data. The quality of a HypoGen model is often best assessed through cost analysis.

### Data Set

Pharmacophore modeling hinges on the correlation between activities and the spatial

arrangement of diverse chemical features within a set of active analogues. For this study, a series of mTOR inhibitors published in recent years was gathered to ensure both structural diversity and a wide activity range. Specifically, 297 human mTOR inhibitors with activity spans (IC<sub>50</sub>) of 0.0016-11000 nM were selected. This initial group was then divided into a training set and a test set.

- **Training Set:** Comprising 24 molecules, this set was thoughtfully crafted for structural diversity and a broad activity spectrum. Molecules with K<sub>i</sub>, ED<sub>50</sub>, EC<sub>50</sub>, and similar activity types were disregarded. The training set plays a pivotal role in pharmacophore generation, determining the resultant model's quality.
- **Test Set:** Encompassing the remaining 273 molecules, this set gauges the generated pharmacophore's predictive capacity. It incorporates highly active, moderately active, and inactive compounds to discern crucial information about mTOR inhibition's pharmacophoric requisites.

A quantitative pharmacophore model was created using a minimum of 0 and a maximum of 4 features—hydrophobic acceptor (HBA), hydrophobic donor (HBD), hydrophobic aliphatic, and ring aromatic (RA). These features were utilized to build hypotheses with an uncertainty value of 3. Quality assessment relied on fixed cost, null cost, total cost, and other statistical measures. A significant difference between fixed and null costs, combined with a unit cost of 40-60 bits, suggested a 75-90% probability of experimental-predicted activity correlation. Pharmacophore models should exhibit statistical significance, accurate activity prediction, and successful retrieval of active compounds from databases. Validation involved parameters like cost analysis, test set prediction, enrichment factors, and goodness of fit. Qualitative and quantitative pharmacophore models were generated using Catalyst's HipHop and HypoGen modules, respectively.

### Conformational Analysis

To delve into molecular flexibility, each compound was treated as a collection of conformers representing distinct regions of the accessible conformational space within a specific energy range. The Poling algorithm and CHARMM force field parameters were leveraged to extensively sample each compound's conformational space. This analysis involved an energy threshold of 20 kcal/mol from the lowest energy level, generating a maximum of 250 conformers for compounds showing accurate activity prediction and undergoing subsequent database searching.



## Database Searching

Virtual screening of chemical databases serves as a strategic approach to identify potential novel leads that could be promising for further development. This method has the distinct advantage of easily obtaining compounds for subsequent biological testing compared to de novo design methods. During database searching, a molecule needs to align with all the features of the pharmacophore model, which is employed as a 3D query. Within DS, two database searching options are available: Fast/Flexible and Best/Flexible search. Optimal results are achieved using the Best/Flexible search option for database screening.

## Molecular Docking

Molecular docking, a computationally intensive technique within SBVS (Structure-Based Virtual Screening), evaluates potential protein-ligand complexes based on their calculated binding affinities. Leveraging the target's crystal structure, molecular docking systematically explores ligand conformations and protein-ligand interactions within a designated protein surface area. It has proven effective in identifying active compounds by filtering out those that don't fit the binding sites. When the target's structural information is absent, a homology model can be constructed and employed for molecular docking. In this study, molecular docking was conducted using a homology model of mTOR, executed through the Glide® program. This approach aids in predicting how compounds interact with the target protein, providing insights into potential binding affinities and facilitating the identification of promising candidates for further investigation.

## REWARDS

**Table 1:**

Ligand	G Score	Lipophilic Evdw	PhobEn	PhobEn HB	PhobEn PairHB	H bond	Elect	Site map	Pi Cat	Cl Br	Low Mw
1	-8.05	-3.71	-1.22	-1.5	0	-1.36	-0.82	-0.03	0	0	-0.19
2	-6.61	-3.97	-1.55	0	0	-0.9	-0.11	-0.4	0	0	-0.38
3	-6.14	-4.08	-1.7	0	0	-0.35	-0.13	-0.26	0	0	-0.13
4	-6.04	-4.67	-1.20	0	0	0	-0.23	-0.31	0	0	-0.19
5	-4.85	-3.75	-1.57	0	0	0	-0.06	-0.21	0	0	-0.33

## PENALTIES

**Table 2.**

Ligand	Penalties	HB Penal	PhobicPenal	RotPenal
1	0	0	0.59	0.21
2	0	0	0.49	0.21
3	0	0	0.37	0.15



4	0	0	0.42	0.16
5	0	0	0.88	0.19

### Lipinski's Rule

Lipinski's Rule, a crucial guideline in drug discovery, assesses the drug-likeness of a chemical compound. The adherence of a compound to Lipinski's rule of five serves as an indicator of its potential bioactivity changes. The molecular properties of the compounds were computed using Molinspiration's molecular properties calculator, and the resulting values are presented in Table 3.

**Table 3.**

Compound No.	Log P	Mol. Wt	HBA	HBD	Rotatable Bonds	TPSA	Mol. vol.	No. of Violations
1	3.27	374.4	7	2	4	99.84	329.44	0
2	4.24	333.77	4	0	2	47.78	280.42	0
3	3.72	408.50	7	1	4	81.39	381.64	0
4	3.02	391.43	8	1	4	95.98	348.31	0
5	4.59	350.84	3	0	2	33.20	313.75	0

Abbreviations: Log P - Partition Coefficient, Mol. Wt. - Molecular Weight, HBA - Hydrogen Bond Acceptor, HBD - Hydrogen Bond Donor, TPSA - Total Polar Surface Area, Mol. Vol. - Molar Volume

### Synthesis

The synthesis process involves multiple steps to create the target compounds. Here's a description of the synthesis procedure:

#### Step 1

1. Pyruvic acid (22 ml, 0.25 mol) was mixed with 200 ml of ethanol, and then benzaldehyde (24 ml, 0.236 mol) was added.
2. The mixture was heated to its boiling point.
3. A solution of pure aniline (23 ml, 0.248 mol) in 100 ml of ethanol was slowly added over the course of 1 hour.
4. The mixture was refluxed (continuously boiled) for about 3 hours.
5. After refluxing, the mixture was allowed to stand overnight.

#### Step 2

1. A previously prepared compound, 2-phenyl-quinoline carboxylic acid (0.01 mole), was taken.

2. To this, 15 ml of thionyl chloride was added.
3. The mixture was refluxed for 30 minutes.
4. Excess unreacted thionyl chloride was removed by heating the reaction mixture on a water bath.

### Step 3

1. The acid chloride product obtained from the previous step was used.
2. It was reacted with various amines, using ethanol as the reaction medium.
3. The mixture was stirred for 5 hours.
4. The resulting mixture was added to cold water, causing a precipitate to form.
5. The precipitate was filtered out.
6. The filtered precipitate was then recrystallized from an appropriate solvent.

The synthesis steps involve the careful combination of reactants and reaction conditions to achieve the desired target compounds. The resulting products are then purified through filtration and recrystallization, ensuring that the synthesized compounds are of suitable quality for further analysis and testing.

### Recrystallization

After the synthesis, the compounds were recrystallized to obtain purified samples:

1. Ethanol was added to the synthesized compound, and the mixture was heated until the compound dissolved completely.
2. The clear solution obtained was immediately filtered to remove any impurities.
3. The filtered solution was set aside to cool.
4. As the solution cooled, crystals of the compound gradually formed.

### Methods for Identification

1. Melting Point: The melting points of the synthesized compounds were determined using the capillary tube method. The temperature at which the compounds started losing their crystalline structure was noted.
2. Thin Layer Chromatography (TLC): A solution of the synthesized compounds in ethanol was prepared. Precoated Aluminium TLC plates were used as the stationary phase, and a developing solvent system of methanol and chloroform (9:1) was used as the mobile phase. The TLC plates were placed in a UV chamber to visualize the spots. Purity of the compounds was confirmed by the presence of a single spot and the absence of secondary

spots.

### Characterization

1. Melting Points: The synthesized compounds exhibited sharp melting points, indicating their crystalline nature.
2. Thin Layer Chromatography (TLC): TLC analysis confirmed the purity of the synthesized compounds by showing a single spot for each compound.
3. IR Spectroscopy: Infrared (IR) spectra of the synthesized molecules were recorded using an ABB Spectrophotometer. The IR spectra provided information about the functional groups present in the compounds within the range of 4000 to 400  $\text{cm}^{-1}$ .
4. Proton NMR Spectroscopy: Proton Nuclear Magnetic Resonance (NMR) spectra were recorded using deuterated methanol as the solvent on a BRUKER advance III 500 NMR spectrometer. The chemical shifts were reported in parts per million (ppm).
5. MASS Spectrometry: The MASS spectra of the synthesized compounds were recorded on a JEOL GC Mate II Mass Spectrophotometer using the Electron Ionization (EI) technique.

### In Vitro Anti-Cancer Activity

The in vitro anti-cancer activity of the synthesized compounds was evaluated using the human colorectal carcinoma cell line (HCT116). Here's the procedure.

followed for the cell treatment and the MTT assay:

### Cell Treatment Procedure

1. The human colorectal carcinoma cell line (HCT116) was obtained from the National Centre for Cell Science (NCCS), Pune.
2. The cells were grown in Dulbecco's Modified Eagles Medium (DMEM) containing 10% fetal bovine serum (FBS).
3. Cells were maintained at 37°C, 5% CO<sub>2</sub>, 95% air, and 100% relative humidity.
4. Cells were detached with trypsin- ethylenediaminetetraacetic acid (EDTA) to create single-cell suspensions.
5. Viable cells were counted using a hemocytometer and diluted with medium containing 5% FBS to achieve a final density of  $1 \times 10^5$  cells/ml.
6. 100 microliters per well of cell suspension were seeded into 96- well plates at a density of 10,000 cells/well and incubated to allow for cell attachment.
7. After 24 hours, cells were treated with serial concentrations of the synthesized

compounds. Different concentrations were used by diluting the compounds in serum-free medium to achieve final concentrations of 100, 10, 1.0, and 0.1  $\mu\text{M}$ .

8. Plates were incubated for 48 hours under appropriate conditions.
9. The medium without samples served as a control. Triplicates were maintained for all concentrations.

### MTT Assay

1. MTT (yellow, water-soluble tetrazolium salt) was used in the assay.
2. A mitochondrial enzyme in living cells, succinate-dehydrogenase, cleaves the tetrazolium ring in MTT, converting it into an insoluble purple formazan compound.
3. The amount of formazan produced is directly proportional to the number of viable cells.
4. After 48 hours of incubation with the compounds, 15  $\mu\text{l}$  of MTT (5mg/ml) in phosphate buffered saline (PBS) was added to each well and incubated for 4 hours.
5. The medium with MTT was removed, and the formazan crystals were solubilized in 100  $\mu\text{l}$  of DMSO (Dimethylsulfoxide).
6. Absorbance at 570 nm was measured using a microplate reader.
7. The percentage of cell inhibition was determined using the formula:  
$$\% \text{ Cell Inhibition} = 100 - (\text{Abs}(\text{sample}) / \text{Abs}(\text{control})) \times 100.$$
8. Nonlinear regression graphs were plotted between % Cell Inhibition and Log10 concentration, and the IC<sub>50</sub> (half-maximal inhibitory concentration) was determined using GraphPad Prism software.

## RESULTS AND DISCUSSION

### 5.1 Pharmacophore Model and Validation

The pharmacophore model developed in this study aimed to predict the activities of active compounds and perform effective database searching.

Two validation methods, the Test Set Prediction method and the Cat- Scramble method, were employed to assess the reliability of this model.

- **Test Set Prediction Method:** This validation method verified the predictive power of the pharmacophore model for compounds not included in the training set. It successfully predicted the activities of these compounds.
- **Cat-Scramble Method:** The Cat- Scramble method, based on Fischer's randomization test, assessed the correlation between chemical structures and biological activity. The results indicated that the model's features significantly correlated with the compounds'

activity.

These validation procedures confirmed the robustness and reliability of the pharmacophore model, indicating its potential to guide the design of new anticancer compounds.

### 5.1.1 Statistical Parameters

Table 4 presents the statistical parameters from the screening of test set molecules, which included the following information:

- Total compounds in the database.
- Total number of active compounds.
- Total hits (active compounds identified).
- Active hits.
- Percentage yield of active compounds.
- Percentage ratio of actives in the hitlist.
- Enrichment factor (Enhancement).
- False negatives.
- False positives.
- GH score (Goodness of Hit list). The GH score, which ranged between 0.7 and 0.8 for the best models, signified a very good model. This information confirms the accuracy and reliability of the pharmacophore models.

### 5.1.2 Pharmacophore Models

Table 5 and 6 present the details of the pharmacophore models generated by HypoGen. The most successful models consistently featured Hydrogen Bond Acceptor (HBA), Hydrogen Bond Donor (HBD), Hydrophobic (HY), and ring aromatic (RA) features.

For cost analysis, the difference between fixed and null costs was considered. A difference  $\geq 70$  bits between these costs indicates a high degree of significance, while a difference greater than 60 bits suggests a true correlation with the data.

These results highlight the robustness and validity of the generated pharmacophore models, emphasizing the importance of specific features in determining the activity of the compounds. This information will be pivotal in guiding further drug design efforts to ensure that newly synthesized compounds adhere to the established pharmacophore characteristics associated with anticancer activity.

Table 5: Outhypo 17.

Hypo.No.	Total cost	Fixed cost	Cost difference	RMSD	Correlation	Features	Max. fit
1	117.729	99.7202	22.872	1.2249	0.836	HBA, HBA, HY, HY, HY	10.1229
2	117.824	99.7202	22.777	1.2217	0.837	HBA, HBA, HY, HY, HY	10.9338
3	117.875	99.7202	22.726	1.2296	0.834	HBA, HBA, HY, HY, HY	9.7913
4	118.19	99.7202	22.411	1.2383	0.832	HBA, HBA, HY, HY, HY	9.443
5	118.755	99.7202	21.846	1.2593	0.825	HBA, HBD, HBD, HY	8.0423
6	118.76	99.7202	21.841	1.2387	0.833	HBA, HBA, HY, HY, HY	11.6888
7	118.946	99.7202	21.655	1.2654	0.824	HBA, HBD, HBD, HY	8.1714
8	120.155	99.7202	20.446	1.3005	0.813	HBA, HBA, HBA, HY	8.6328
9	120.875	99.7202	19.726	1.3216	0.806	HBA, HBD, HBD, HY	8.7544
10	120.949	99.7202	19.652	1.3281	0.804	HBA, HBA, HY, HY, HY	9.4722

Table 6: Outhypo 1.

Hypo. No.	Total cost	Fixed cost	Cost difference	RMSD	Correlation	Features	Max. fit
1	123.316	98.8074	17.285	1.4290	0.7685	HBA, HBD, HBD, HYALI	7.9201
2	123.765	98.8074	16.836	1.3811	0.7932	HBD, HYALI, RA, RA	10.4565
3	123.767	98.8074	16.834	1.3173	0.8263	HBA, HBD, RA	8.6055
4	124.173	98.8074	16.428	1.4517	0.7601	HBA, HBD, HBD, HYALI	8.4634
5	124.504	98.8074	16.097	1.4289	0.7723	HBD, HBD, HYALI, RA	9.8660
6	124.735	98.8074	15.866	1.4691	0.7533	HBA, HBA, HBD, HYALI	8.2707
7	124.811	98.8074	15.79	1.4425	0.7666	HBD, HBD, HYALI, RA	9.7348
8	124.845	98.8074	15.756	1.4266	0.7750	HBD, HYALI, RA, RA	10.1712
9	124.846	98.8074	15.755	1.4065	0.7856	HBD, HYALI, RA, RA	10.5895
10	125.056	98.8074	15.545	1.4697	0.7532	HBD, HBD, HYALI, RA	8.9747

## 5.2 Docking Studies

Molecular docking experiments were conducted to position the ligands within the active sites of the mTOR protein. This crucial step ensured that the ligands interacted effectively with the protein.

Active sites were identified as binding sites within the protein structure. The docking process systematically searched for the best conformations and orientations for the ligands within these binding sites. Scoring and energy optimization helped exclude undesirable poses, and Monte Carlo Sampling refined the conformations. Energy minimization using the OPLS-2001 force field further improved the docking poses.

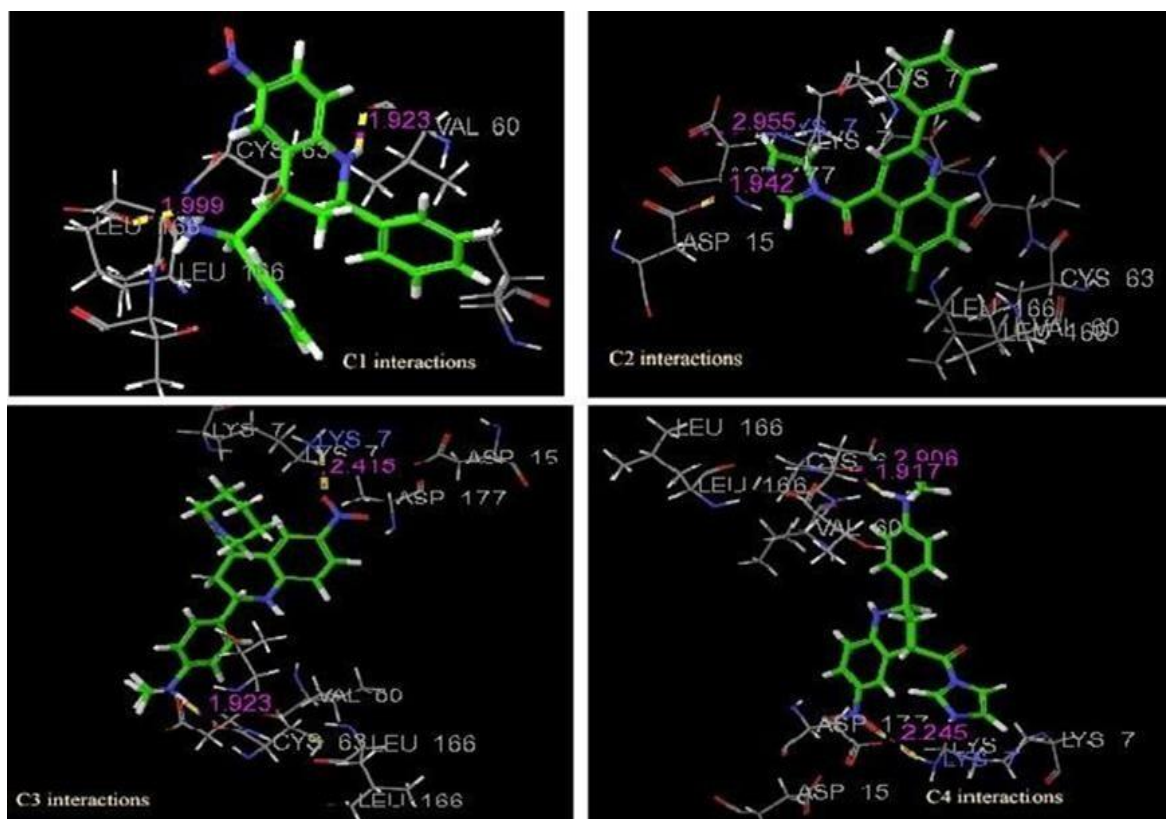


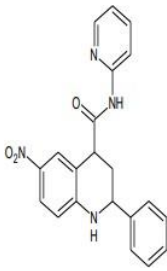
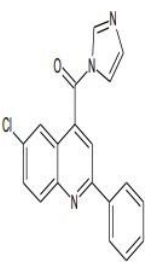
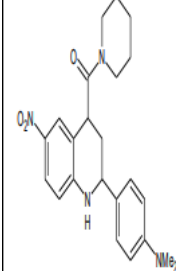
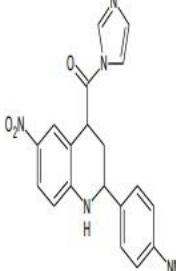
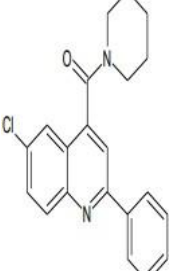
**Fig. 11: Interactions.**

The results showed that each ligand established hydrogen bond interactions with key amino acids, including Aspartic acid 64, Aspartic acid 177, Lysine 7, Valine 60, Glycine 64, and Aspartic acid 15. This demonstrates the essential role of these hydrogen-bonding amino acids in inhibiting mTOR activity. This information will be invaluable in guiding the design of compounds that target the mTOR protein effectively.

### 5.3 Synthesis and Characterization

The synthesis and characterization results for each compound are presented in Table 9. This table provides information about the recrystallization method, yield, melting point, TLC parameters, and spectral data (IR, NMR, and MASS) for each compound.



Compoundno.	C-1	C-2	C-3	C-4	C-5
Structure					
Recrystallization	Ethanol	Ethanol	Ethanol	Ethanol	Ethanol
Yield (%)	76	78	75	80	77
Melting Point	76 <sup>0</sup> C	90 <sup>0</sup> C	212 <sup>0</sup> C	214 <sup>0</sup> C	32 <sup>0</sup> C
TLC	Precoated Silica-gel GFplates	Precoated Silica-gel GF plates	Precoated Silica-gel GF plates	Precoated Silica-gel GF plates	Precoated Silica-gel GF plates
Stationary Phase					
Mobile Phase	Methanol	Methanol	Methanol	Methanol	Methanol
Spots Location	UV Chamber	UV Chamber	UV Chamber	UV Chamber	UV Chamber
IR spectroscopy (cm <sup>-1</sup> )	1304(C-N)	756(C-Cl)	1319(C-N)	1319(C-N)	764(C-Cl)
	1474(ArC=C)	1311(ArC-N)	1373 cm-	1373 cm-	1311(ArC-N)
	1597(C-NO2)	1628(ArC=C)	1(N(CH3)2)	1(N(CH3)2)	1497(ArC=C)
	1636(C=O)	1674(C=O of	1458(ArC=C)	1458(ArC=C)	1674(C=O of Amide)
	2962(ArC-H)	Amide)	1551(C-NO2)	1551(C-NO2)	2978(ArC-H)
	3479(N-H)	2932(ArC-H)	1651(C=O)	1643(C=O)	
			3070(ArC-H)	3063(ArC-H)	
NMR	16(4 H)	6.6(3H,Ar)	2.4(6H,N(CH	2.4(4H)	
spectroscopy	6.1(4H, Ar)	7.5(5H,Ar)	3)	3.3(6H,N(CH3))	1.6(10H)
	6.6(4H, Ar)	7.9(3H,Het.Ar)	2.9(4H)	6.2-6.9(7H,Ar)	6.1,6.4,6.6(8H,Ar)
	7.2(1, NH)	8.4(1H,Het.Ar)	3.2(10H)	7.6-	7.9(1H,Het.Ar)
	8.1(4H,Het.Ar)		7.0(1H,NH)	7.9(3H,Het.Ar)	
	9.9(1H, NH)		7.6-9.6(7H,Ar)	9.7(1H,NH)	
MASS	374.41(M+,6%)	333.38(M+,12	408.52(M+,6	391.42(M+,7%)	350.88(M+,10%)
Spectrometry		61.77(B,100%)	%)	135.21(B,100%)	62.57(B,100%)
			61.77(B,100%)		
	140.30(B,100				
	%				

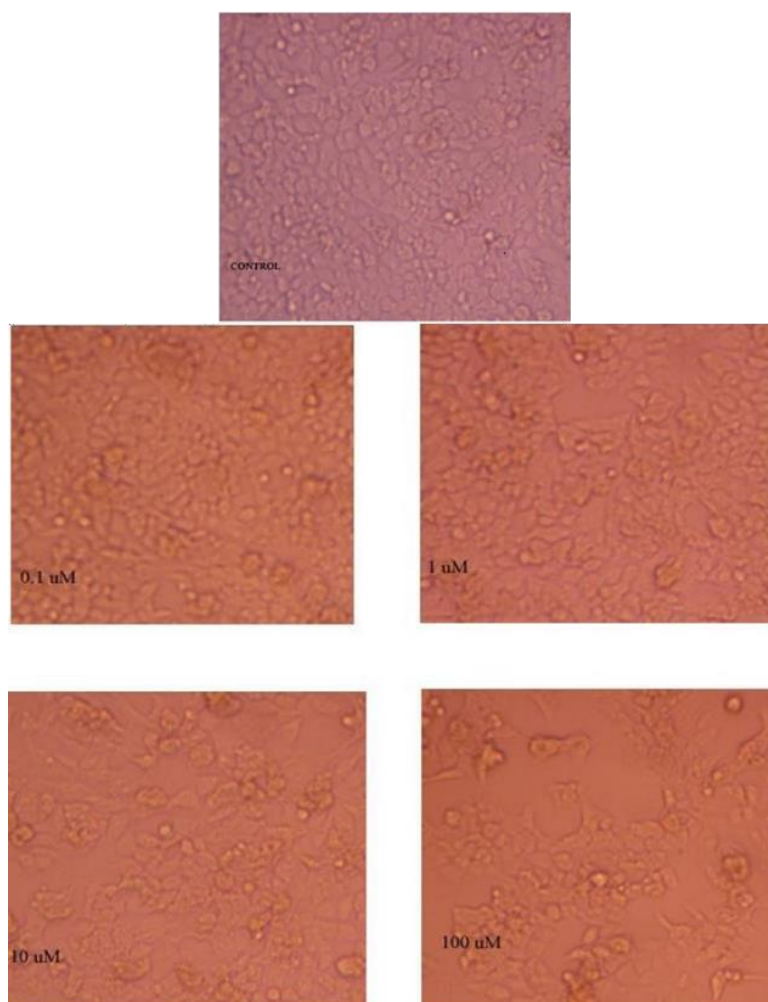
#### 5.4 Cytotoxicity Studies

Cytotoxicity studies were performed on the synthesized compounds. The results revealed the IC<sub>50</sub> values, which indicate the concentration required to inhibit 50% of cell growth. The compounds, particularly compound 1 and 2, showed significant effects on human colorectal carcinoma cells (HCT 116), with IC<sub>50</sub> values of 97.38 and 113.2  $\mu$ M/ml, respectively. The high R<sup>2</sup> values (0.9911 and 0.9979) indicate the reliability of these findings.

In conclusion, the pharmacophore model and docking studies demonstrated the validity and potential of the designed models in identifying anticancer compounds. Moreover, the

successful synthesis and characterization of compounds, coupled with the promising results of cytotoxicity studies, pave the way for the development of novel and effective anticancer agents. These findings hold promise for the advancement of anticancer drug discovery and the improvement of treatments for colorectal carcinoma.

### Compound 1



	Conc. $\mu\text{M/ml}$	Absorbance	% inhibition	IC <sub>50</sub> $\mu\text{M/ml}$	R <sup>2</sup>
C1	0.1	0.564333	1.684088	97.38	0.9911
	1	0.526	8.362369		
	10	0.473333	17.53775		
	100	0.281	51.0453		

### SUMMARY AND CONCLUSION

In this research endeavor, the focus was on the design and evaluation of potential anticancer compounds targeting the mTOR protein. The following key findings and conclusions have been drawn from the study:

**Docking and Screening:** A comprehensive computational approach was employed, utilizing drug design software (Maestro 9.1), to dock candidate molecules and assess their potential anticancer activity against the mTOR protein. Among the evaluated compounds, twenty-five scaffolds displayed high docking scores against the mTOR inhibitor, meeting the criteria of Lipinski's rule.

**Selection of Quinoline Scaffold:** From the pool of potential compounds, a scaffold containing the quinoline nucleus was selected based on its synthetic feasibility, suggesting that it could serve as a promising lead compound for further research.

**Characterization:** All synthesized compounds underwent rigorous characterization through various spectroscopic techniques, including UV spectroscopy, IR spectroscopy, NMR spectroscopy, and MASS spectrometry. The compounds were confirmed to be of high purity.

**In Vitro Anticancer Activity:** In vitro experiments were carried out using the MTT assay procedure to assess the anticancer activity of the synthesized compounds against the mTOR inhibitor. The results demonstrated the effectiveness of the compounds in inhibiting cancer cell growth.

In conclusion, this research represents a significant step towards the development of novel anticancer compounds targeting the mTOR protein. The compounds demonstrated high docking scores, low toxicity profiles, and promising in vitro anticancer activity. To advance these findings into potential clinical applications, further studies, including organ toxicity and in vivo anticancer assessments, are imperative. Ultimately, these investigations aim to establish the synthesized compounds as safe and effective agents for cancer treatment with a low side effect profile.

## BIBLIOGRAPHY

1. Momna Hejmadi. Introduction to cancer biology. Ventus Publishing ApS, 2010; 6-13.
2. Cancer [Online]. Available from: <https://www.cancer.gov/about-cancer/understanding/what-is-cancer> [Accessed on 21 July, 2023].
3. B. Ganesh, Sanjay D. Talole, Rajesh Dikshit, A case-control study on diet and colorectal cancer from Mumbai, India. Cancer Epidemiology, 2009; 33: 189-93.
4. Rajaraman Swaminathan, Ramanujam Selvakumaran, Pulikattil Okkuru Esmey, P. Sampath, Jacques Ferlay, Vinoda Jissa, Viswanathan Shanta, Cancer pattern and survival

- in a rural district in South India. *Cancer Epidemiology*, 2009; 33: 325–31.
5. J. Cardoso, J. Boer, H. Morreau, R. Fodde, Expression and genomic profiling of colorectal cancer. *Biochimica et Biophysica Acta*, 2007; 103–37.
  6. H.E. Blum, Colorectal Cancer: Future Population Screening for Early Colorectal Cancer. *Eur. J. cancer*, 1995; 31A: 1369-72.
  7. Suzanne Hector, Jochen H.M. Prehn, Apoptosis signaling proteins as prognostic biomarkers in colorectal cancer: A review. *Biochimica et Biophysica Acta*, 2009; 117–29.
  8. Laura Asnaghi, Paola Bruno, Marcella Priulla, Angelo Nicolini, mTOR: a protein kinase switching between life and death. *Pharmacological Research*, 2004; 50: 545– 49.
  9. David A. Guertin and David M. Sabatini, Defining the Role of mTOR in Cancer. *Cancer Cell*, 2007; 12: 9-22.
  10. JB Easton and PJ Houghton, mTOR and cancer therapy. *Oncogene*, 2006; 25: 6436– 46.
  11. Carlos Garcia-Echeverria, Allosteric and ATP-competitive kinase inhibitors of mTOR for cancer treatment. *Bioorg. & Med. Chem. Lett.*, 2010; 20: 4308-12.
  12. mTOR pathway [Online]. Available from: [www.abcam.com](http://www.abcam.com) [Accessed on 21 July, 2023].
  13. Yap, T. A., Garrett, M. D., Walton, M. I., Raynaud, F., De Bono, J. S., & Workman, P. Targeting the PI3K–AKT–mTOR pathway: Progress, pitfalls, and promises. *Current Opinion in Pharmacology*, 2008; 8(4): 393-412. <https://doi.org/10.1016/j.coph.2008.08.004>
  14. Margit Rosner, Michaela Hanneder, Nicol Siegel, Alessandro Valli, Christiane Fuchs, Markus Hengstschlager, The mTOR pathway and its role in human genetic diseases. *Mut. Res.*, 2008; 659: 284-92.
  15. Dos D Sarbassov, Siraj M Ali and David M Sabatini, Growing roles for the mTOR pathway. *Current Opinion in Cell Biology*, 2005; 17: 596–603.
  16. Jie Chen, Yimin Fang, A novel pathway regulating the mammalian target of rapamycin (mTOR) signaling. *Biochemical Pharmacology*, 2002; 64: 1071-77.
  17. Venselaar H, Krieger E, Vriend G. Homology modeling. *Structural Bioinformatics*, 2009; 5(4): 715-32.
  18. Koji Ogata and Hideaki Umeyama, An automatic homology modeling method consisting of database searches and simulated annealing. *J. Mol. Graphics Mod.*, 2000; 18: 258–72.
  19. Anthony Ivetac and J. Andrew McCammon. A Molecular Dynamics Ensemble- Based Approach for the Mapping of Druggable Binding Sites. In: Riccardo Baron, editor. *Computational drug discovery and design, methods in molecular biology*. USA: Humana Press, 2012; 3-9.

20. Daniel Seeliger, Bert L. de Groot, Ligand docking and binding site analysis with PyMOL and Autodock/Vina. *J. Comp. Aided Mol. Des.*, 2010; 24: 417-22.
21. Povl Krogsgaard-Larsen, Tommy Liljefors and Ulf Madsen. *Textbook of Drug Design and Discovery*. 3rd ed. London and New York: Taylor & Francis, 2005.
22. Lipinski C.A, Lombardo F, Dominy B.W and Feeney P.J. Experimental and Computational approaches to estimate solubility and permeability in drug discovery and development settings. *Adv. Drug Delivery Rev.*, 1997; 23(1-3): 3-25.
23. Kitchen DB, Decornez H, Furr JR, Bajorath J, Docking and scoring in virtual screening for drug discovery: methods and applications. *Nature reviews, Drug discovery*, 2004; 3(11): 935-49.
24. Lengauer T, Rarey M, Computational methods for biomolecular docking. *Curr. Opin. Struct. Biol.*, 1996; 6(3): 402-6.
25. Solomon V R, Lee H, Quinoline as a privileged scaffold in cancer drug discovery. *Curr. Med. Chem.*, 2011; 18(10): 1488-508.
26. Karunakar Tanneeru, Lalitha Guruprasad, Ligand-based 3-D pharmacophore generation and molecular docking of mTOR kinase inhibitors. *J. Mol. Model.*, 2011.
27. Drug design [Online]. Available from: [www.celgene.com/research/drug\\_discovery\\_and\\_development.aspx](http://www.celgene.com/research/drug_discovery_and_development.aspx) [Accessed on 24 July, 2023].
28. Drug design [Online]. Available from: [www.scfbio\\_iitd.res.in/tutorial/drugdiscovery.htm](http://www.scfbio_iitd.res.in/tutorial/drugdiscovery.htm) [Accessed on 24 July, 2023].
29. Catalyst, version 4.11; Accelrys Inc: San Diego, CA 92121, USA, 2010.
30. Cerius2, version 4.11; Accelrys Inc: San Diego, CA 92121, USA, 2010.
31. Catalyst [Online]. Available from: [http://accelrys.com/products/datasheets/pharmacophore\\_modelling.pdf](http://accelrys.com/products/datasheets/pharmacophore_modelling.pdf) [Accessed on 24 July, 2023].
32. Glide version 9.1, Schrodinger, L.L.C., New York, 2010.
33. Graham L. Patrick. *An introduction to medicinal chemistry*, 4th ed. Oxford university press, 2008; 683-84.
34. Molecular properties [Online]. Available from: [www.molinspiration.com](http://www.molinspiration.com) [Accessed on 26 July, 2023]
35. A.I. Vogel, A.R. Tatchell, B.S. Furnis, A.J. Hannaford, P.W.G. Smith. *Vogel's textbook of practical organic chemistry*. 5th ed. New Delhi: Prentice Hall, 2007; 1187.
36. Hiren M. Marvaniya, Palak K. Parikh and Dhruvo Jyoti Sen, Synthesis and *in-vitro* screening of 3,4-dihydropyrimidin-2(1*H*)-one derivatives for antihypertensive and calcium channel blocking activity. *J. App. Pharm. Sci.*, 2011; 1(5): 109-13.

37. Mostafa M. Ghorab, Fatma A. Ragab, Mostafa M. Hamed, Design, synthesis and anticancer evaluation of novel tetrahydroquinoline derivatives containing sulfonamide moiety. *European Journal of Medicinal Chemistry*, 2009; 44: 4211–17.
38. Yue-Ling Zhao, Yeh-Long Chen, Feng- Shuo Chang , Cherng-Chyi Tzeng, Synthesis and cytotoxic evaluation of certain 4-anilino-2- phenylquinoline derivatives. *Eur. J. Med. Chem.*, 2005; 40: 792–97.
39. Afshin Zarghi, Razieh Ghodsi, Design, synthesis, and biological evaluation of ketoprofen analogs as potent cyclooxygenase-2 inhibitors. *Bioorg. Med. Chem.*, 2010; 18: 5855–60.
40. K.D. Thomas, Airody Vasudeva Adhikari, Sandeep Telkar, Imran H. Chowdhury, Riaz Mahmood, Nishith K. Pal, Guru Row, E. Sumesh, Design, synthesis and docking studies of new quinoline-3-carbohydrazide derivatives as antitubercular agents. *European Journal of Medicinal Chemistry*, 2011; 46: 5283-92.
41. Gurdeep R. Chatwal, Sham K. Anand. *Instrumental methods of Chemical Analysis*. 5th ed. Himalayan Publishing House, 2005; 2: 196-226.
42. Sharma B.K. *Instrumental methods of Chemical Analysis*. Meerut: Goel Publishing House, 1994.
43. Skoog, West Holler, Crouch. *Fundamental of Analytical Chemistry*. 8th ed. Singapore: Thomson Books/Cole, 2008; 710-40.
44. Acute oral toxicity [Online]. Available from: URL:[http://ccvam.niehs.nih.gov/SuppDocs/Feld Docs/OECD/OECD\\_GL423.pdf](http://ccvam.niehs.nih.gov/SuppDocs/Feld Docs/OECD/OECD_GL423.pdf) [Accessed on 29 July, 2023]
45. Mosmann T, Rapid colorimetric assay for cellular growth and survival: application to proliferation and cytotoxicity assays. *Journal of Immunological Methods*, 1983; 65: 55-63.
46. Anne Monks, Dominic Scudiero, Philip Skehan, Robert Shoemaker, Kenneth Paull, David Vistica, Curtis Hose, John Langley, et.al., Feasibility of high flux anticancer drug screen using a diverse panel of cultured human tumour cell lines. *Journal of the National Cancer Institute*, 1991; 83(11): 757-66.
47. Arjan A. van de Loosredicht, Esther Nennie, Gert J. Ossenkoppele, Robert H.J. Beelen, and Mart M.A.C. Langenhuijsen, Cell mediated cytotoxicity against U 937 cells by human monocytes and macrophages in a modified colorimetric MTT assay. *J. Immunological Methods*, 1991; 141: 15-22.
48. Ichiro Miki, Naomi Ishihara, Masanari Otoshi and Hiroshi Kase, Simple colorimetric cell-cell adhesion assay using MTT stained leukemia cells. *J. Immunological Methods*,



- 1993; 164: 255-61.
49. Rajesh Kakadiya, Huajin Dong, Amit Kumar, Dodia Narsinh, Xiuguo Zhang, Ting- Chao Chou, Te-Chang Lee, Anamik Shah, Tsann-Long Su, Potent DNA-directed alkylating agents: Synthesis and biological activity of phenyl N-mustard–quinoline conjugates having a urea or hydrazinecarboxamide linker. *Bioorg. & Med. Chem.*, 2010; 18: 2285–99.
50. Afshin Zarghi, Razieh Ghodsi, EbrahimAzizi, Bahram Daraie, Mehdi Hedayati, Orkideh G. Dadrass, Synthesis and biological evaluation of new 4-carboxyl quinoline derivatives as cyclooxygenase-2 inhibitors. *Bioorg. & Med. Chem.*, 2009; 17: 5312–17.
51. Andrew N. Boa, Shane P. Canavan, Paul R. Hirst, Christopher Ramsey, Andrew M. W. Stead, and Glenn A. McConkey, Synthesis of brequinar analogue inhibitors of malaria parasite dihydroorotate dehydrogenase. *Bioorg. & Med. Chem.*, 2005; 13: 1945–67.
52. Ya-Yun Lai, Li-Jiau Huang, Kuo-Hsiung Lee, Zhiyan Xiao, Kenneth F. Bastow, Takao Yamoric and Sheng-Chu Kuo, Synthesis and biological relationships of 30,6- substituted 2- phenyl-4 quinolone-3-carboxylic acid derivatives as antimitotic agents. *Bioorg. & Med. Chem.*, 2005; 13: 265–75.